



Published in final edited form as:

Nature. 2015 October 8; 526(7572): 268–272. doi:10.1038/nature14908.

Dilution of the cell cycle inhibitor Whi5 controls budding yeast cell size

Kurt M. Schmoller¹, J.J. Turner¹, M. Kõivomägi¹, and Jan M. Skotheim^{1,*}

¹Department of Biology, Stanford University, Stanford, CA 94305, USA

Abstract

Cell size fundamentally affects all biosynthetic processes by determining the scale of organelles and influencing surface transport^{1,2}. Although extensive studies have identified many mutations affecting cell size, the molecular mechanisms underlying size control have remained elusive³. In budding yeast, size control occurs in G1 phase prior to *Start*, the point of irreversible commitment to cell division^{4,5}. It was previously thought that activity of the G1 cyclin Cln3 increased with cell size to trigger *Start* by initiating the inhibition of the transcriptional inhibitor Whi5⁶⁻⁸. However, while Cln3 concentration does modulate the rate at which cells pass *Start*, we found that its synthesis increases in proportion to cell size so that its total concentration is nearly constant during pre-*Start* G1. Rather than increasing Cln3 activity, we identify decreasing Whi5 activity — due to the dilution of Whi5 by cell growth — as a molecular mechanism through which cell size controls proliferation. Whi5 is synthesized in S/G2/M phases of the cell cycle in a largely size-independent manner. This results in smaller daughter cells being born with higher Whi5 concentrations that extend their pre-*Start* G1 phase. Thus, at its most fundamental level, budding yeast size control results from the differential scaling of Cln3 and Whi5 synthesis rates with cell size. More generally, our work shows that differential size-dependency of protein synthesis can provide an elegant mechanism to coordinate cellular functions with growth.

To control size, proliferating cells tie division to growth. However, the molecular mechanisms by which growth triggers division are poorly understood^{3,9,10}. In the budding yeast *Saccharomyces cerevisiae*, which divides asymmetrically into a larger mother and smaller daughter cell, size control takes place in the first G1 phase of daughter cells^{5,11,12}. Progression through G1 is promoted by the upstream G1 cyclin Cln3 in complex with the cyclin-dependent kinase Cdk1. This Cln3-Cdk1 complex is thought to partially inactivate the transcriptional inhibitor Whi5^{13,14}. Inactivation of Whi5 relieves inhibition of the transcription factor SBF, whose transcriptional activation completes a positive feedback loop committing the cell to division⁴. While its upstream position in the G1 regulatory network suggests that Cln3 is the trigger, its concentration does not clearly increase during G1^{8,15}. This leads to the question of why G1 progression is size-dependent when the putative trigger protein Cln3 does not increase in concentration.

Users may view, print, copy, and download text and data-mine the content in such documents, for the purposes of academic research, subject always to the full Conditions of use:http://www.nature.com/authors/editorial_policies/license.html#terms

*address correspondence to skotheim@stanford.edu.

Author Contribution: All authors designed experiments and wrote the manuscript; KMS, JT and MK performed experiments.

Two prevailing models propose mechanisms to generate a size-dependent signal from the constant Cln3 concentration. One model proposes that the increasing number of Cln3 molecules is titrated against the fixed number of SBF-binding sites on the genome⁶. This DNA-titration serves to convert the constant Cln3 concentration to an increasing activity at its target sites on the genome. The other model proposes that Cln3 is retained at the endoplasmic reticulum and is rapidly released upon sufficient growth-dependent accumulation of the chaperone Ydj1^{7,16}. Here, we perform a series of experiments whose results are inconsistent with the two existing models. Instead, we identify a new molecular mechanism for cell size control that does not require Cln3 activity increasing with cell size. Rather, we show that cell size promotes G1 progression by diluting Cln3's primary target, Whi5 (Fig. 1a).

To determine how the G1 regulatory network implements size control, we first examined how the concentration of key regulators changes through G1. We grew cells using ethanol as the carbon source to generate small daughter cells subject to strong cell size control⁵. We restricted our attention to these daughter cells, and used time lapse microscopy to measure the concentration of proteins tagged with the fluorescent protein mCitrine and expressed from the endogenous locus (Fig. 1b-g; Extended Data Fig. 1a). The concentration of wild-type Cln3 cannot be measured with this approach due to its rapid and constitutive degradation. We therefore examined two mutants expressing stabilized proteins (*CLN3-11A* and *CLN3-1*¹⁷⁻¹⁹; Extended Data Fig. 1b). Consistent with previous bulk measurements of wild-type Cln3, Cln3-11A and Cln3-1 concentrations are constant through G1 (Fig. 1b). Moreover, we observed no changes in Cln3-11A localization (Extended Data Fig. 2). This is inconsistent with the Cln3 retention model, which predicts a rapid increase in nuclear Cln3 concentration in mid-G1⁷. Similarly, the concentrations of the key G1 regulators Swi4, Whi3, and Bck2 are nearly constant through G1 (Fig. 1c-e). In sharp contrast, we found that the concentration of the cell cycle inhibitor Whi5 strongly decreases through G1 (Fig. 1f, Extended Data Fig. 3a). This implies that the dilution of the cell cycle inhibitor Whi5 could serve as the size-dependent signal promoting cell cycle progression (Fig. 1a). Such an inhibitor-dilution model²⁰ represents a qualitatively distinct mechanism of cell size control that does not require a size-dependent increase in Cln3-activity.

While inhibitor dilution explains how growth drives proliferation, it does not immediately explain why smaller-born cells grow more in G1. This would also require that smaller-born cells start G1 with a higher concentration of Whi5. Indeed, we found that the concentration of Whi5 at cell birth monotonically decreases with cell size, whereas the concentration of Cln3-11A and Cln3-1 at cell birth is independent of cell size (Fig. 2a-b). We confirmed that Whi5 is diluted in G1 using quantitative immunoblots (Fig. 2c). Finally, for a given birth size, diploid cells are born with a much higher Whi5 concentration (Fig. 2d, Extended Data Fig. 4a), which is consistent with the long-standing observation that cell size scales linearly with ploidy^{3,21}. Taken together, our data support a size control model in which all cells are born with a similar dose of Whi5, which they dilute by growth to progress through G1.

Inhibitor-dilution results in size-dependent cell cycle progression because smaller cells are born with higher Whi5 concentrations. To identify the origin of this size-dependent Whi5 concentration, we measured the rate of Whi5 synthesis throughout the cell cycle. We found

that Whi5 is a stable protein, synthesized primarily during S/G2/M (Fig. 2d, Extended Data Fig. 3b, 5a), consistent with previous mRNA measurements²². Whi5 is differentially partitioned so that, following division, concentration in daughter cells is consistently higher than in mother cells (Extended Data Fig. 6a-b). Critically, during S/G2/M, Whi5 is synthesized at a rate largely independent of cell size (Fig. 2e-f, Extended Data Fig. 3b, and 4b). Since S/G2/M duration weakly depends on mother cell size (Extended Data Fig. 6c), small and large cells produce similar amounts of Whi5. This results in larger budded cells having a lower Whi5 concentration just before division (Extended Data Fig. 6d). Since larger mother cells produce larger daughter cells (Extended Data Fig. 6e), this explains the inverse correlation between Whi5 concentration and cell size at birth, which is essential for the inhibitor-dilution size control model.

The size-independent synthesis rate of Whi5 during S/G2/M shows it is not limited by the general biosynthetic capacity of the cell, which increases with cell size. This contrasts with the expectation that transcriptional and translational outputs scale with cell size²³. Indeed, mCitrine-Cln3-11A synthesis in G1 is proportional to cell size (Fig. 2g; Extended Data Fig. 5b-c). Thus, the differential size scaling of Cln3 and Whi5 synthesis lies at the heart of cell size control in budding yeast.

Since ploidy is an important determinant of cell size, we decided to examine how it impacts the differential synthesis of Cln3 and Whi5. As expected for the majority of genes, whose synthesis is limited by the biosynthetic capacity of the cell, Cln3-11A synthesis in a diploid cell is comparable to the synthesis of a similarly sized haploid cell, despite having two copies of *mCitrine-CLN3-11A* (Fig. 2g). Thus, in diploids the biosynthetic machinery is split between the two copies of the genome. Consistently, a hemizygous diploid synthesizes mCitrine-Cln3-11A protein at a much lower rate than a similarly sized haploid or homozygous diploid (Fig. 2g). In sharp contrast, Whi5-mCitrine synthesis is similar and size-independent in hemizygous diploid and haploid cells (Fig. 2f, Extended Data Fig. 4b). Moreover, a homozygous diploid produces Whi5 at approximately twice the rate, similar to a haploid with two copies of *WHI5* (Fig. 2f, Extended Data Fig. 4b). Thus, the rate of Whi5 synthesis is determined by the number of copies of the gene and is independent of cell size and ploidy.

While the inhibitor-dilution model takes into account cell-to-cell variability in birth size, it does not yet include the fact that cells born the same size will vary in how much they grow before *Start*⁵ (Fig. 3a). For a population of similarly sized pre-*Start* cells, only a fraction will pass *Start* within the short time interval between movie frames. This allows us to define a rate as this fraction divided by the time interval (Fig. 3b; see Methods). In our inhibitor-dilution model, the rate at which cells pass *Start* is determined by the concentrations of Whi5 and Cln3. If Cln3 concentration is constant in pre-*Start* cells, the Whi5 concentration alone should predict the rate at which cells progress through *Start*. To test this model, we generated haploid strains containing 1, 2, and 4 copies of *WHI5-mCitrine*. We note these experiments are in a *bck2Δ* background, where Cln3 is essential²⁴. As expected, cells containing 2 and 4 copies of *WHI5* produced proportionally more Whi5 protein, were larger, and exhibited a decreased size-dependent rate of progression through *Start* (Fig. 3b, Extended Data Fig. 4c-d). We note that these experiments were performed using cells

expressing wild type *CLN3*, which is suggested to be at constant concentration in G1 based on our measurements of Cln3-11A and Cln3-1. In complete agreement with an inhibitor-dilution model with a size-independent activator, the concentration of Whi5 alone predicts the rate at which cells progress through *Start* for all 3 strains (Fig. 3c). Consistently, the relationship between the rate of progression through *Start* and Whi5 concentration was not changed in *hcm1Δ* cells that lack a transcription factor promoting *WHI5* expression²² (Extended Data Fig. 7).

In our inhibitor-dilution model, Cln3 concentration determines the fraction of active Whi5. Thus, for a given Whi5 concentration, it should be possible to drive cell cycle entry by sufficiently increasing Cln3 concentration. To test these predictions, we constructed a *bck2Δ* strain that carries *mCitrine-CLN3-11A* under control of the methionine-regulated *MET25* promoter. In this strain, repressing *CLN3-11A* expression arrests cells in G1, during which they continue to grow. Thus, by first arresting cells for varying durations and then inducing *CLN3-11A* for varying lengths of time, we were able to examine a wide range of cell sizes and Cln3 and Whi5 concentrations (Fig. 4a). We binned cells by size, which determines Whi5 concentration, and performed a logistic regression to determine the critical Cln3 concentration (pulse amplitude that results in half the cells budding; e.g., Fig. 4b, Extended Data Fig. 8). Larger cells required lower Cln3-11A concentrations to enter the cell cycle (Extended Data Fig. 8d), consistent with previous results showing that larger G1 cells were more sensitive to Cln1 expression²⁵. Next, we used a strain that carries *MET25pr-CLN3-11A* and *WHI5-mCitrine* to measure the average Whi5 concentration as a function of cell size under the same arrest conditions (Extended Data Fig. 8e). The critical Cln3 concentration increases with Whi5 concentration as predicted by the Whi5-dilution model (Fig. 4c).

The Whi5-dilution model, unlike DNA-titration models, does not explicitly depend on the DNA content of the cell and predicts that the relationship between the critical Cln3 concentration and Whi5 concentration should be independent of ploidy. To test this, we repeated the same set of pulsing experiments using diploid strains and found a similar relationship between the critical Cln3 and Whi5 concentrations (Fig. 4c; $p > 0.05$). This is consistent with experiments showing that introducing heterologous DNA through yeast artificial chromosomes does not affect progression through G1²⁶. However, we note that increased ploidy delays progression through S/G2/M, which results in larger daughter cells and mean population size (Fig. 2f; Extended Data Fig. 9).

To determine that the relevant parameter for *Start* is Whi5 concentration, rather than cell size, we repeated the pulse experiments with a strain that carries a hormone inducible promoter expressing a *WHI5-mCherry* allele in addition to the *MET25pr-mCitrine-CLN3-11A* allele (Fig. 4d). This allowed us to generate cells of different sizes containing similar Whi5 concentrations. As predicted, the probability of a cell passing *Start* increases with Cln3 concentration ($p < 10^{-5}$), decreases with Whi5 concentration ($p < 10^{-5}$), but is independent of cell size ($p > 0.5$) (Fig. 4e).

Taken together, our data support a new inhibitor-dilution model for size control in budding yeast. In this model, cell growth dilutes the cell cycle inhibitor Whi5 to drive progression through the cell cycle, whereas Cln3 concentration remains constant. Nevertheless,

condition-specific regulation of Cln3 transcription²⁷, translation²⁸, or stability²⁹ likely modulates cell size. For the inhibitor-dilution mechanism to control cell size, it is crucial that the amount of Whi5 that cells are born with not scale with size. In contrast, the cell cycle activator Cln3 is produced in proportion to size. This differential size-dependency of cell cycle activator and inhibitor synthesis constitutes the basis of budding yeast size control (Fig. 4f).

Inhibitor-dilution is an elegant mechanism to control cell size independently of other aspects of cell geometry. In rod shaped cells, such as fission yeast and bacteria, geometric mechanisms measuring lengths or surface areas can sensitively measure cell size because these metrics are directly proportional. However, such geometric measurements would perform poorly in near-spherical budding yeast, where intra-cellular lengths scale with cube root of cell volume, so that a doubling of cell size results in only a ~25% increase in characteristic length. Geometric mechanisms are also unlikely to be applicable to more irregularly shaped metazoan cells. In contrast, inhibitor-dilution mechanisms can measure cell volume with no geometric constraints. All that is required is the differential size scaling of a cell cycle activator relative to an inhibitor. Due to the simplicity of this requirement, we anticipate the wide application of inhibitor-dilution mechanisms to control cell size.

Methods

Imaging and image analysis

All experiments were performed using a CellASIC microfluidics device with Y04C plates. A Zeiss Observer Z1 microscope with an automated stage using a plan-apo 63X/1.4NA oil immersion objective was used to take images every 3 minutes. Focusing was performed using automated Definite Focus hardware. Strains expressing mCitrine fusion proteins were exposed for 400 ms using the Colibri 505 LED module at 25% power. Whi5-mCherry was imaged by exposure for 500 ms using the Colibri 540-80 LED module at 50% power. Under these illumination conditions, we did not observe detectable photobleaching (Extended Data Fig. 10a). Cell and nuclear segmentation and quantification of fluorescence signals was performed as in³⁰. We subtracted the size-dependent autofluorescence signal as determined from comparable experiments with unlabelled strains (Extended Data Fig. 10b-c) to measure the total fluorescence intensity in single cells from fluorescent-fusion proteins. Total fluorescence intensity is proportional to the protein amount. To determine protein concentration, we calculate cell volume from the phase image segmentation by assuming rotational symmetry around the major axis in the xy-plane. We confirmed that localization of Whi5 did not significantly affect concentration measurements (Extended Data Fig. 3c,d).

Experimental design and statistical analysis

All data shown were obtained from at least 2 independent experiments. For each experiment, we collected data from 10-20 imaging positions. Comparison of biological replicates allowed us to assay for systematic errors. This resulted in sufficient data for our statistical comparisons.

Cell cycle phase analysis

After automated segmentation, we manually annotated pedigrees and determined time points of cell birth, bud emergence, and cytokinesis from phase images. We only included daughter cells that were born during the experiment in our analyses. For cells shown in Fig. 1 and 2, we estimated G1 using cytokinesis and bud emergence. Whi5 enters the nucleus ~9 minutes before cytokinesis⁵, which can also be detected by visual inspection of phase images. For Fig. 3, we estimated the time of *Start*, the point of commitment to cell division beyond which haploid cells no longer arrest in response to an abrupt exposure to a high concentration of mating pheromone. *Start* in haploid cells corresponds to the point where ~50% of the peak nuclear Whi5 has been removed from the nucleus⁴. *Start* takes place ~12 minutes before the full exit of Whi5-mCitrine from the nucleus in cells growing on 2% glycerol and 1% ethanol. For *2xWHI5-mCitrine* and *4xWHI5-mCitrine* strains, we used 12 minutes before full Whi5 exit as a proxy for *Start*.

Whi5 and Cln3 synthesis rate estimates

To estimate Whi5 synthesis rates, we analyzed time series for the amount of Whi5-mCitrine in the S/G2/M phase of the cell cycle (the budded phase). This phase was determined as described above. We fit a line to the data and took the slope as an estimate of the Whi5 synthesis rate because Whi5 is a highly stable protein (Extended Data Fig. 5a). Synthesis rate estimates for individual cells are plotted against the cell size at the time of bud emergence (Extended Data Fig. 4b), mean values for size-binned data are shown in (Fig. 2f). We used a similar method to estimate the much lower Whi5 synthesis rate during G1 (Extended Data Fig. 3b).

To estimate Cln3 synthesis rates during G1, we analyzed time series for individual cells expressing mCitrine-Cln3-11A. For each cell, we estimate the Cln3-11A synthesis rate, k , over a 30-minute interval in which we assume it is constant. This is valid because a cell growing on glycerol/ethanol changes little in size during a 30-minute interval. We excluded cells with G1 durations shorter than 30 minutes. We assume protein degradation can be characterized by an exponential decay constant $\tau \sim 83$ minutes that we independently measured (Extended Data Fig. 5c). We take N to be the number of Cln3-11A molecules, so

that $\frac{dN}{dt} = k - \frac{1}{\tau}N$, which can be solved to yield the number of Cln3-11A molecules $N = N_0 e^{-t/\tau} + k\tau (1 - e^{-t/\tau})$. Here, N_0 denotes the amount of Cln3 at the beginning of the interval. N_0 and k are then determined from fitting this equation to the data. The synthesis estimate k is then plotted against the cell size at the beginning of the interval (Fig. 2g).

Estimate of rate at which cells pass *Start*

The *Start* transition is a highly stochastic process⁵, which means that cells born at the same size will vary in how much time they spend growing in pre-*Start* G1. Thus, for a population of similarly sized pre-*Start* cells, only a fraction will pass *Start* within a given time interval. To quantify this phenomenon, we calculate the fraction of pre-*Start* cells within a size interval that pass *Start* within one frame of our movie (3 minutes). Thus, we define the rate at which cells pass *Start* as a function of cell size as the fraction of cells within the size bin

that passed *Start* divided by the time interval between movie frames. Similarly, we can also define the rate at which cells pass *Start* as a function of Whi5 concentration by grouping cells by Whi5 concentration rather than cell size. We note that the *Start* transition is defined in the cell cycle phase analysis section above based on⁴. This analysis, based on binning cells by size or Whi5 concentration, was used to obtain the jagged lines in Fig. 3b,c. The smooth curves, and associated 95% confidence intervals, were obtained by logistic regression of the unbinned dataset as follows. For each frame, a pre-*Start* cell is described by 3 numbers: cell size, Whi5 concentration, and whether or not that cell passed *Start* in the next 3 minutes (= 1 if the cell passed *Start*; otherwise = 0). Data from all time points for all pre-*Start* daughter cells were pooled into a large matrix with 3 columns. We then performed a logistic regression using the MATLAB function *glmfit* to estimate the probability of a cell passing *Start* as a function of either cell size or Whi5 concentration.

We note that Fig. 3C shows that the instantaneous probability for a cell to pass *Start* is determined by the Whi5 concentration, not volume. However, this does not necessarily mean that cells with different Whi5 copy number need to reach the same Whi5 concentration. Consider two cells born with different Whi5 concentrations. The one with the higher Whi5 concentration has to grow for a certain amount of time to reach the initial Whi5 concentration of the second cell. Since the probability for passing *Start* is always non-zero, there is a certain chance that the cell enters the cell cycle even before reaching the birth concentration of the one with lower Whi5 concentration. Thus, on average, cells born with higher initial Whi5 concentrations will pass *Start* at higher Whi5 concentrations. Adding an extra copy of Whi5 does result in an increase of cell size, however, cell size is not doubled. Thus, $2xWHI5$ cells are on average born with higher Whi5 concentrations, but also pass *Start* at higher Whi5 concentrations, even though the *instantaneous* probability to pass *Start* as a function of Whi5 is the same as in wildtype cells.

We also note that the series of experiments described in figures 3 and 4 were performed in a *bck2Δ* background. In the absence of Cln3, Bck2 drives large cells into the cell cycle²⁴. However, since Bck2 concentration is constant through G1 (Fig. 1e), and the targets of this transcriptional regulator extend across the entire cell cycle^{31,32}, we decided to focus exclusively on the Cln3-Whi5 mechanism, which is specific for G1 progression, and performed subsequent analyses in a *bck2Δ* background.

Cln3 pulse experiments

For the experiments shown in Fig. 4, cells were grown on media lacking methionine, SCD-Met (*MET25pr-mCitrine-CLN3-11A* on). After 150 minutes of growth in the microfluidic device, 10x methionine was added to arrest cells in G1 (*MET25pr-mCitrine-CLN3-11A* off). After varying arrest times (2, 3 or 4 hours for haploids, 3 hours for diploids) methionine was removed for 0, 30, 40, 50, or 60 minutes (20, 30, 40, or 50 minutes for diploids) to induce a pulse of mCitrine-Cln3-11A expression. For daughter cells born during the experiment, we determined whether or not the cell budded during a 2 hour time window following the onset of *CLN3-11A* induction. In addition, we measured the maximum Cln3-11A concentration. Cell size was measured at the time of maximum Cln3-11A concentration. For each strain, we then pooled all the data (22 independent experiments for haploids, 6 for diploids) and

binned cells according to their size. For each size bin we used a logistic regression to calculate the critical mCitrine-Cln3-11A concentration where 50% of the cells bud. In order to determine the median Whi5 concentration as a function of cell size we arrested *MET25pr-CLN3-11A bck2Δ WHI5-mCitrine* cells and measured Whi5 concentration as a function of cell size during the arrest (Extended Data Fig. 8). Error bars for Fig. 4c were calculated as the maximum of the 95% confidence interval of the logistic regression and the estimated experimental error due to variation in fluorescence intensity from experiment to experiment. We used a linear regression model to test whether ploidy affects the relationship between Whi5 and critical Cln3-11A concentrations. For the experiments shown in Fig. 4e and Extended Data Fig. 8, we used a hormone inducible *LexApr*³³ to express a *Whi5-mCherry* allele to decouple cell size and Whi5 concentration. We induced Whi5 by addition of β -estradiol (30-100 nM) for at least 6 hours, and removed β -estradiol prior to the experiment. This allowed us to generate cells of varying size and Whi5 concentration by varying the induction level of Whi5 and the duration of G1 arrest (2, 2.5 or 3 hours; 18 independent experiments) prior to the Cln3-11A pulse induction in SCD-Met.

Growth conditions

For microscopy-based experiments, yeast were grown in synthetic complete (SC) media with 2% glycerol and 1% ethanol except for the pulse experiments shown in Fig. 4, where yeast were grown on SC media with 2% glucose. Before an imaging experiment, cells were grown to an OD <0.1 after which they were sonicated for ~5s at 3W intensity. For quantitative immunoblots, cells were grown on SC 2% galactose 2% raffinose overnight before being arrested in SC 2% glucose.

Strains and plasmids

All strains were congenic with W303 (see Table S1), and were constructed using standard methods. See Table S2 for plasmid list. To enable fluorescent Cln3 detection in live cells, it was necessary to use a stabilized variant of the protein. Stabilizing Cln3 by removing its degradation-inducing phosphosites¹⁷ (Cln3-10A) allowed direct observation of Cln3-10A-mCitrine. However, induction of this stabilized variant with the *MET25* promoter resulted in severe cytokinesis defects. We therefore added an additional mutation (R108A), which was reported to increase protein stability, but reduce the ability of Cln3 to drive cell cycle progression¹⁸. Also, R108A has been examined in the context of the double mutant K106A R108A (see variant Cln3-A10 in³⁴) that increased steady state protein levels, but was less able to rescue a *cln1Δ cln2Δ cln3Δ bck2Δ* strain. Cln3-A10 was also reported to decrease the interaction with Cdc28 in³⁵ (where it is known as the *Cln3-A13* mutation). Combining the 10 stabilizing alanine mutations from¹⁷ with the R108A mutation from¹⁸ resulted in a stabilized, less active Cln3 protein (Extended Data Fig. 1b), which we refer to as Cln3-11A, whose concentration and amount were measurable in single cells without disrupting cytokinesis. For Fig. 1b and 2a, we measured the concentration of Cln3 protein expressed from a previously characterized stabilized C-terminal truncation allele *CLN3-1*^{19,36}.

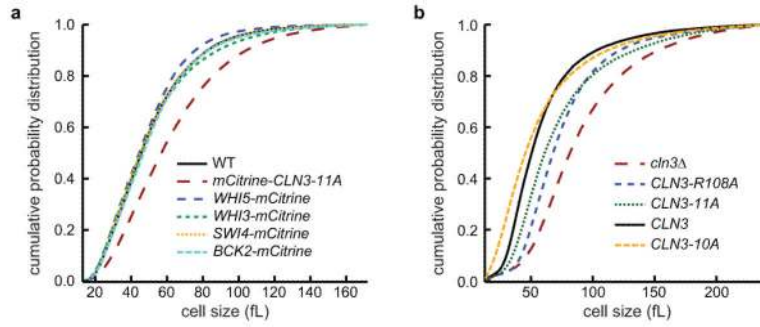
Quantitative Whi5 Immunoblot

Strain JTY6 (*cln1Δcln2Δcln3Δ GAL1pr-CLN1 WHI5-3xFLAG*) was generated using plasmid pMK15 digested with MluI (New England BioLabs Inc, USA). Cells were grown at 30° to mid-log phase (OD₆₀₀ 0.2) in synthetic complete media with 2% galactose and 2% raffinose before being washed once and resuspended in an equal volume of SC with 2% glucose and incubated for 120 minutes at 30°C. 10 mL samples were removed every 30 minutes for 150 minutes, and then every 45 minutes for 90 minutes thereafter. Samples were pelleted and frozen in liquid nitrogen. Concurrently, 1 mL samples were removed, sonicated, and analyzed with a Coulter Z2 cell counter to measure cell size distributions with size cutoffs set at 30 and 500 fL.

Frozen cell pellets were thawed on ice, resuspended in 200 μL urea lysis buffer (20 mM Tris•Cl pH 7.5, 7M urea, 2M thiourea, 65 mM CHAPS, 65 mM DTT, 50 mM NaF, 100 mM beta-glycerophosphate, 1 mM NaVO₃, 1 mM PMSF), and homogenized for 40 seconds at 4° in a FastPrep homogenizer (MP Biomedicals) using an equal volume of 0.5mm diameter ceramic beads. Cell lysates were transferred to fresh microfuge tubes by puncturing the bottom of the tubes used for lysis, placing them in fresh tubes, and centrifuging for a few seconds at low speed. Lysates were then cleared by centrifuging at 17,000g for 10 minutes. Total protein concentration in the lysates was determined by Bradford analysis, and samples were diluted to a maximum volume of 12 μL in urea buffer, of which 10 μL were mixed with 5 μL 6x Laemmli sample buffer and run on a 12% (29:1) polyacrylamide gel. Gels were cut to include only the relevant molecular weight range, and proteins from all gels were transferred to a nitrocellulose membrane using program 8 for 7 minutes on an iBlot dry transfer device (Thermo Fisher Scientific). Membranes were blocked in Licor Odyssey blocking buffer (TBS; 927-50010) for 30 minutes at room temperature. Membranes were incubated with 1:1000 M2 mouse monoclonal anti-FLAG (Sigma F1804) and 1:5000 rat monoclonal anti-tubulin YOL1/34 (Abcam ab6161) diluted in Licor Odyssey blocking buffer + 0.2% Tween-20 for 60 minutes, and they were washed 1× 15 minutes and 3× 5 minutes in TBS + 0.1% Tween-20. Membranes were then incubated in 1:15,000 goat anti-mouse conjugated to Alexa Fluor 680 (Thermo Fisher Scientific A-21058) and goat anti-rat conjugated to Licor IRDye 800CW (Licor Inc., 925-32219) in the same buffer as for primary antibodies and washed as before. Membranes were imaged in a Licor Odyssey CLX-0670.

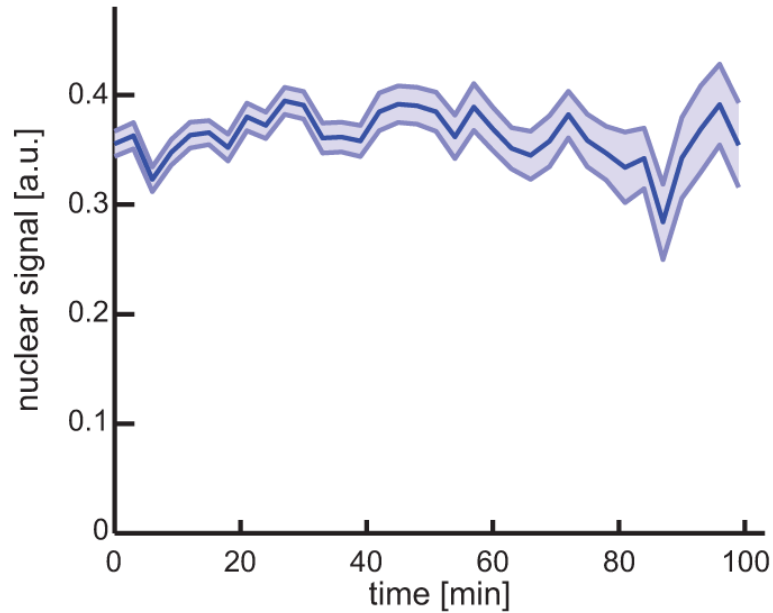
Immunoblot images were analyzed by manually specifying band boundaries and measuring total intensity using Licor Image Studio Light. Background regions for each lane were also specified manually. These values were used to generate background-subtracted values, which were analyzed with respect to mean population size using R.

Extended Data



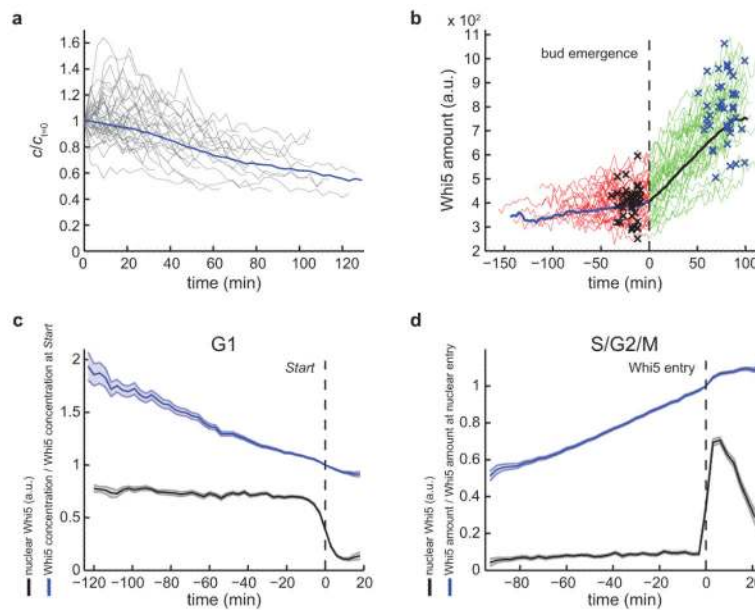
Extended Data Figure 1. Size distributions of strains expressing mCitrine fusion proteins or *CLN3* mutant alleles

a. Cell size distributions were measured in a Coulter Counter for 5 strains expressing the indicated mCitrine fusion proteins from the endogenous locus and a wild type control. These 5 strains were used in Figure 1. All strains were grown on SC 2% glycerol, 1% ethanol. **b.** Size distributions measured using a Coulter Counter for *cln3Δ* cells expressing *CLN3* alleles from a *CLN3* promoter integrated at the *URA3* locus. See methods for description of *CLN3* mutant alleles. Cells were grown on SC 2% glucose.



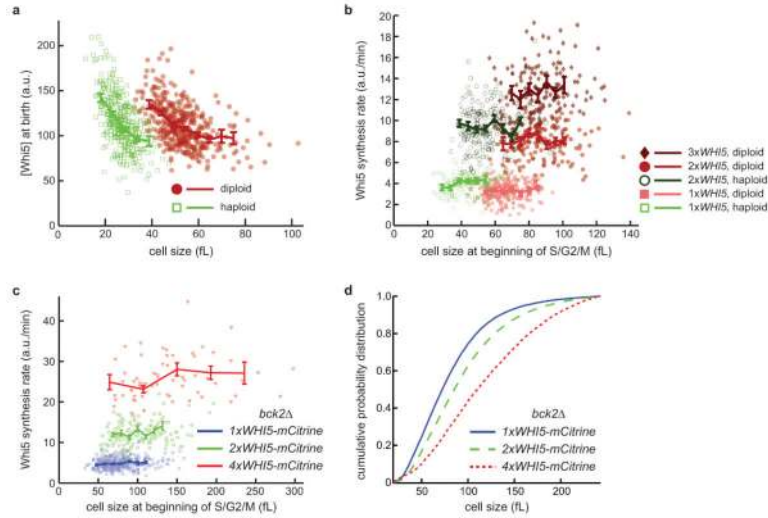
Extended Data Figure 2. mCitrine-Cln3-11A is consistently nuclear during G1

We see no evidence of a rapid re-localization of Cln3-11A into the nucleus at mid-G1 (n=471). Nuclear signal measured and nucleus segmented as described in³⁰. Thick line denotes mean and shaded area denotes standard error of the mean.



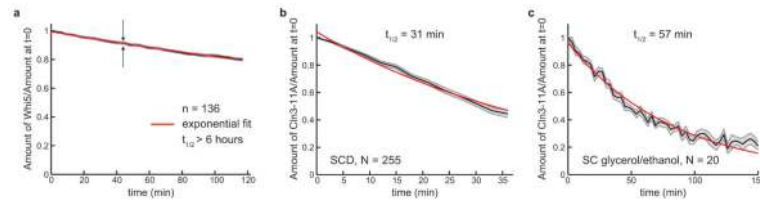
Extended Data Figure 3. Single cell analysis of Whi5 dilution and synthesis

a, We randomly selected 40 out of 339 single cell traces that correspond to the data shown in Fig. 1f for display here. The relative change of Whi5 concentration during G1 is shown in grey (thin lines). Blue thick line shows the mean of all 339 cells. **b**, We randomly selected 40 out of 147 single cell traces of Whi5 amount for display. Traces are aligned by bud emergence ($t=0$). G1 (cell birth to bud emergence) is shown in red (mean of all 147 cells is shown in blue). S/G2/M (bud emergence to cytokinesis) is shown in green (mean is shown in black). Black X's denote time points of full nuclear Whi5 exit, blue X's denote time points of full nuclear Whi5 reentry. The rate of synthesis of Whi5 in S/G2/M phase is 6.6-fold higher than in G1 phase. 89% of total Whi5 in this experiment is synthesized in S/G2/M. **c-d**, Control for the effect of Whi5 localization on concentration measurements. Rapid relocalization of Whi5 at *Start* **c**, and just before cytokinesis **d**, does not affect concentration measurements. **c**, Mean relative change of cellular Whi5 concentration during G1 aligned by *Start* (50% nuclear Whi5 exit as determined from a logistic fit to the nuclear signal) and standard error of the mean are shown in blue. The corresponding nuclear Whi5 signal is shown in black (mean and standard error of the mean; nuclear signal measured and nucleus segmented as described in ³⁰). $n=320$. **d**, Mean relative change of cellular Whi5 amount during S/G2/M in mother-bud pairs aligned by the time point of 50% Whi5 entry into the nucleus (as determined from a logistic fit to the nuclear signal) and standard error of the mean are shown in blue. The corresponding nuclear Whi5 signal is shown in black (mean and standard error of the mean; nuclear signal measured and nucleus segmented as described in ³⁰). $n=133$. Cells express Whi5-mCitrine from the endogenous locus. Cells were grown on SC 2% glycerol, 1% ethanol.



Extended Data Figure 4. Whi5 concentration and synthesis rate

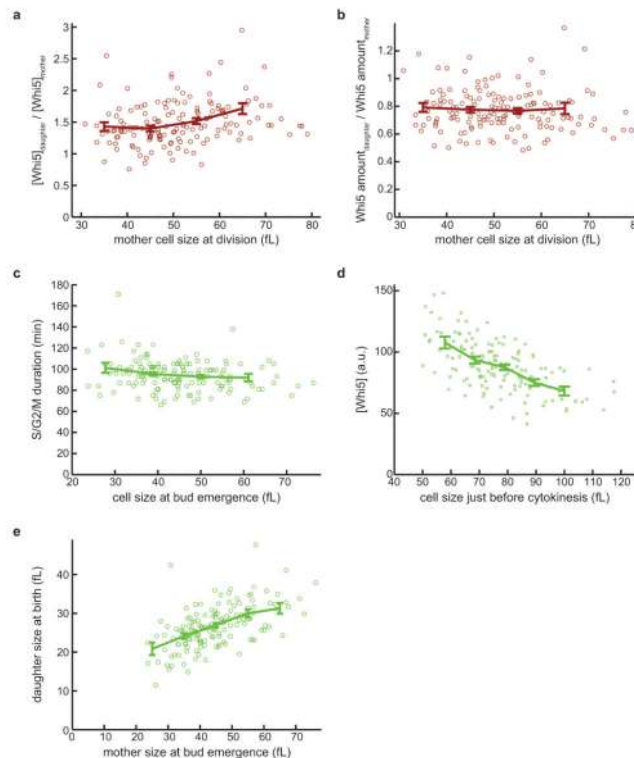
Single cell data corresponding to Fig. 2d and 2f. **a**, Whi5 concentration at cell birth is shown as a function of cell size for individual haploid ($n=339$) and diploid ($n=385$) cells. **b**, The rate of Whi5 synthesis as a function of cell size for each genotype as indicated. **c**, The rate of Whi5 synthesis as a function of cell size for *bck2Δ* strains expressing 1, 2 or 4 copies of *WHI5-mCitrine* ($n=353$, 129 and 66, respectively). Bars denote mean values and standard errors. **d**, Cell size distributions measured using a Coulter Counter for the indicated strains. Cells were grown on SC 2% glycerol 1% ethanol.



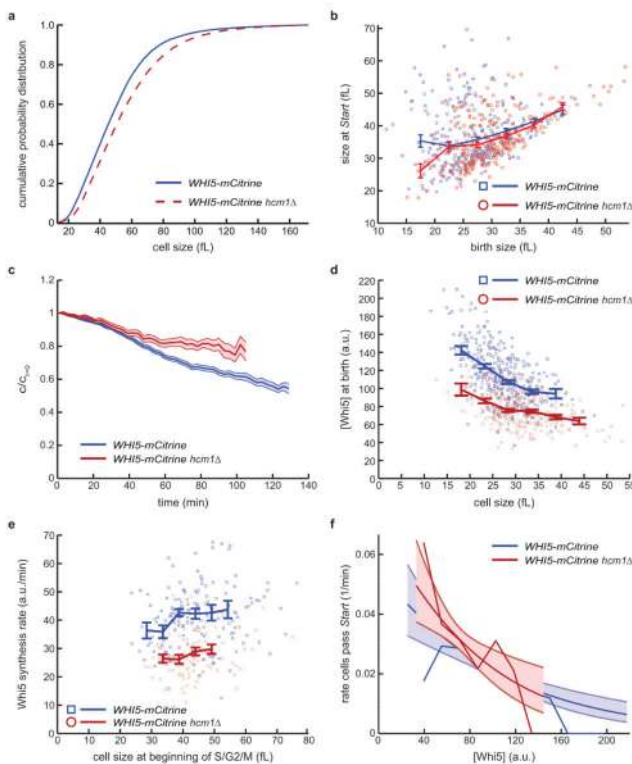
Extended Data Figure 5. Whi5 and Cln3-11A stability

a, Whi5-mCherry was expressed from a hormone inducible promoter³³ (*LexApr-WHI5-mCherry*), which was inactivated prior to the experiment (see Fig. 4d-e). The mean amount of Whi5-mCherry in G1 phase daughter cells was measured for each cell relative to its amount at $t=0$. The distance between the black arrows indicates the standard error of the mean. We estimated a half-life > 6 hours for cells grown in SC 2% glucose. **b-c**, mCitrine-Cln3-11A was expressed from a *MET25* promoter for **(b)** 1 hour on SC-Met 2% glucose or **(c)** >4.5 hours on SC-Met 2% glycerol 1% ethanol. Next, transcription was inactivated by switching cells to media composed of either **(b)** SC +10x methionine 2% glucose or **(c)** SC 2% glycerol 1% ethanol +10x methionine. So that the cells had sufficient time to inactivate protein synthesis, we began our protein half-life measurement 21 minutes (33 minutes for SC 2% glycerol 1% ethanol) after methionine addition. Data and exponential fit shown for daughter cells in G1 phase. Black line indicates means and gray area indicates standard error of the mean. The short half-life of Cln3-11A relative to the doubling time of cell volume together with the constant concentration of Cln3-11A through G1 (Fig. 1-2), implies that

Cln3-11A synthesis is proportional to cell volume. To see this, consider the time-dependent equation for changes in Cln3 concentration $\frac{d[Cln3]}{dt} = \frac{r}{V} - [Cln3] \times (d+g)$, where r is the rate of Cln3 protein synthesis (units of molecules * time⁻¹), V is the cell volume, d is the degradation rate of Cln3 (units of time⁻¹), and g is the rate of dilution of Cln3 due to cell growth (units of time⁻¹). Since [Cln3] is constant, the left hand side = 0. Also, the half-life of Cln3-11A is larger than that of Cln3, but much smaller than the time it takes to double the cell volume (~90 minutes on SCD, ~180 minutes on SC 2% glycerol 1% ethanol) so that $d \gg g$. Thus, the equation simplifies to $0 = \frac{r}{V} - [Cln3] \times d$ so that the rate of Cln3 synthesis is proportional to cell volume, $r = V \times d \times [Cln3]$. This is consistent with our estimates of Cln3-11A synthesis rates shown in Fig. 2g.

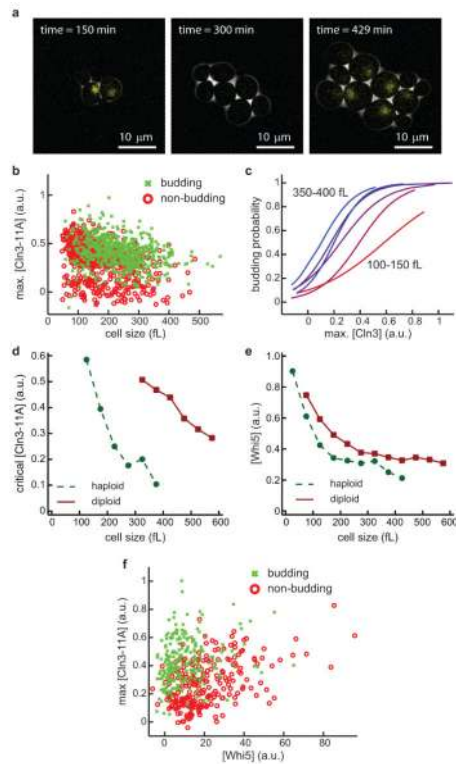


Extended Data Figure 6. Linking Whi5 partitioning and synthesis to concentration at birth
 Daughter cells begin G1 with 1.49 ± 0.03 fold higher concentration of Whi5 than their mother cells. Shown is the ratio of Whi5-mCitrine concentrations (a) and amount (b) for daughter-mother pairs at the beginning of G1 phase. c, The duration of S/G2/M exhibits small, but significant size-dependence ($p < 0.01$). d, The total Whi5 concentration in first-generation mother cells just before cytokinesis decreases as a function of cell size. e, The size of daughter cells is correlated with the size of their mothers at the time of bud emergence. Cells were grown on SC 2% glycerol 1% ethanol. $n=151$. Points denote single cell data. Bars denote mean values and standard error of the mean.



Extended Data Figure 7. Size control and Whi5 synthesis in *hcm1Δ* cells

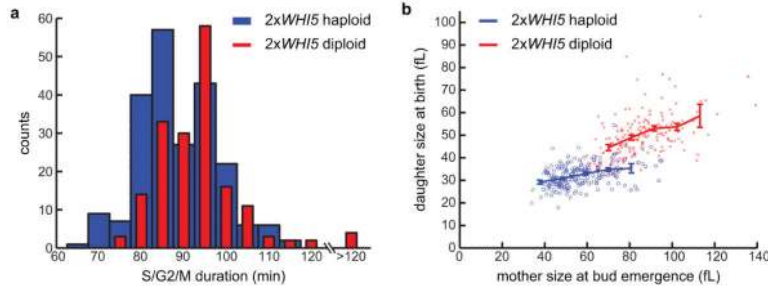
a. Cell size distributions of wild type (blue solid line) and *hcm1Δ* (red dashed line) cells, both carrying a *WHI5-mCitrine* allele, were measured in a Coulter Counter. **b.** Size at *Start* as a function of birth size is shown for wildtype (n=339) and *hcm1Δ* (n=262) daughter cells. Bars denote mean and standard error. Note that small *hcm1Δ* cells exhibit poor size control (leftmost bin). **c.** Change in cellular Whi5 concentration during G1 for daughter cells. Cells are born at t=0 and the change in concentration is shown with standard error of the mean. Blue denotes wildtype (see also Fig. 1f), red denotes *hcm1Δ* cells. **d.** Whi5 concentration at cell birth is shown as a function of cell size for wildtype (n=339) and *hcm1Δ* (n=284) daughter cells. **e.** The rate of Whi5 synthesis as a function of cell size is shown for wildtype (n=151) and *hcm1Δ* (n=106) cells. Bars denote mean values and standard errors. Squares and circles denote single cell data. **f.** The rate at which daughter cells progress through *Start* is shown as a function of Whi5-mCitrine concentration for wild type (blue, n=334) and *hcm1Δ* (red, n=262) cells. Smooth lines are logistic regressions and the corresponding shaded areas denote 95% confidence intervals. Jagged lines connect means for binned data. Cells were grown on SC 2% glycerol 1% ethanol.



Extended Data Figure 8. Data supporting Cln3-11A-pulse experiments shown in Fig. 4

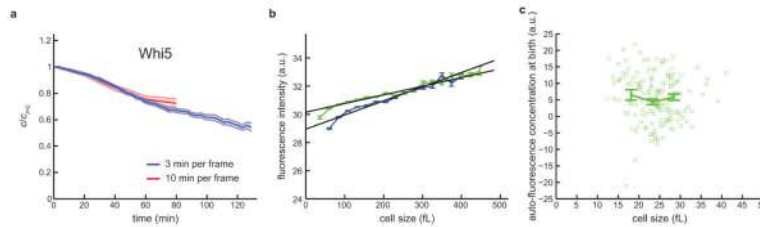
a, composite phase and fluorescence images of *bck2Δ MET25pr-mCitrine-CLN3-11A* haploid cells used in the pulse experiment shown in Fig. 4a-c. Cells were grown in the absence of methionine (*MET25pr-mCitrine-CLN3-11A* on). After 150 minutes (see image), cells were arrested in G1 by addition of 10x methionine to the SCD-Met medium. After variable lengths of arrest (3 hours for the images shown here – see second image), a pulse of Cln3-11A was expressed by removal of methionine from the medium (1 hour pulse for the experiment shown here – see third image). **b**, For daughter cells born during the experiment, we determined the maximum Cln3-11A concentration during the pulse, the corresponding cell volume, and whether or not the cell budded. Data from 22 different experiments were pooled. **c**, Cells were binned according to their size. For each 50 fL size bin we used a logistic regression to calculate budding probability as a function of Cln3-11A peak concentration. **d**, For each size bin, the critical Cln3-11A concentration was determined as the amplitude of the pulse where 50% of the cells budded. A similar set of experiments was done for diploid cells. $n = 1195$ for haploids, and $n = 405$ for diploids. **e**, *bck2Δ MET25pr-CLN3-11A WHI5-mCitrine* cells were arrested in G1 by addition of 10x methionine to the SCD-Met medium. Cells were tracked during the G1 arrest and the median Whi5-mCitrine concentration was measured as a function of size. $n = 162$ for haploids, and $n = 148$ for diploids. **f**, Single cell data corresponding to Fig. 4e. *MET25pr-mCitrine-CLN3-11A LexApr-WHI5-mCherry bck2Δ* haploid cells are used for Cln3-11A pulse experiments to decouple cell size and Whi5 concentration. Maximum Cln3-11A concentration, corresponding cell size and Whi5 concentration, and whether or not the cell budded were determined in 18 independent experiments for a total of 471 daughter cells (see Methods). This generated a 4-dimensional dataset that we used build a logistic regression model. In this

model, we predicted cell cycle entry (budding) using a linear combination of cell size, Whi5 and Cln3-11A. This resulted in a model based solely on Cln3-11A and Whi5. Thus, once Cln3-11A and Whi5 concentrations are measured, cell size yields no additional information. To visualize this result in Fig. 4e, we binned our data into 6 bins based on cell size (greater or less than 295 fl) and Whi5 concentration (<10, 10-25, and 25-40 a.u.). For each of these 6 bins, we performed a logistic regression to estimate the probability of entering the cell cycle as a function of the peak mCitrine-Cln3-11A concentration produced by the pulse.



Extended Data Figure 9. Ploidy increases S/G2/M duration and cell size at birth

a, Histogram showing the duration of S/G2/M for haploid cells containing an extra copy of *WHI5* (blue, n=220) and wild type diploid cells (red, n=176). **b**, The size of daughter cells is shown as a function of the size of their mothers at the time of bud emergence. At a given mother size, diploid cells produce larger daughter cells. Cells were grown on SC 2% glycerol 1% ethanol. Bars denote means and standard error of the mean.



Extended Data Figure 10. Photobleaching control and size-dependent background subtraction

a, The concentration of Whi5-mCitrine decreases during G1 as shown in Fig. 1f. Increasing the time between frames from 3 minutes (n = 339) to 10 minutes (n = 75) did not significantly affect our concentration measurements, indicating that photobleaching of the mCitrine fluorescent protein was not significant in our experiments. **b**, Auto-fluorescent signal in the mCitrine channel during G1 arrest for an unlabeled strain (*bck2Δ MET25pr-CLN3*) in two independent experiments (blue: n = 79, green: n = 89). Cells were grown on SCD+10x methionine. Bars denote mean and standard error of the mean for each size bin. The average of these two experiments was used for background subtraction in Fig. 4. A similar size-dependent background subtraction was performed for each experimental condition and for also for the mCherry red fluorescent channel. **c**, Cell-to-cell variation in background-subtracted autofluorescence concentration measured in an unlabeled cell. One of the experiments with the unlabeled wildtype strain used to determine the auto-fluorescence signal for the experiments shown in Fig.1-3 is analyzed the same way as experiments shown in Fig. 2a and 2b (n = 164). This illustrates cell-to-cell variation in auto-

fluorescence. Due to experiment-to-experiment variation, a single control experiment with an unlabeled strain will typically result in a mean “concentration” of ± 5 a.u. (compared to the average autofluorescence used for analysis), while cell-to-cell variability in autofluorescence within one experiment exhibits a standard deviation of ~ 10 a.u.. Note that the arbitrary units in a) and b) are not comparable, because different settings were used to export the microscopy data for the pulse experiments shown in Fig. 4.

Supplementary Material

Refer to Web version on PubMed Central for supplementary material.

Acknowledgements

We thank Oguzhan Atay and Jessica Feldman for reagents, Rob de Bruin, Amy Gladfelter, Martha Cyert, and Mart Loog for comments on the manuscript, the Burroughs Wellcome Fund (CASI), the NSF (CAREER), NIH training grant GM007276 (JJT), and HFSP (KMS and MK) for funding.

Bibliography

- Goehring NW, Hyman AA. Organelle growth control through limiting pools of cytoplasmic components. *Curr Biol.* 2012; 22:R330–9. [PubMed: 22575475]
- Chan Y-HM, Marshall WF. Scaling properties of cell and organelle size. *Organogenesis.* 2010; 6:88–96. [PubMed: 20885855]
- Turner JJ, Ewald JC, Skotheim JM. Cell size control in yeast. *Curr Biol.* 2012; 22:R350–9. [PubMed: 22575477]
- Doncic A, Falleur-Fettig M, Skotheim JM. Distinct Interactions Select and Maintain a Specific Cell Fate. *Mol Cell.* 2011; 43:528–539. [PubMed: 21855793]
- Di Talia S, Skotheim JM, Bean JM, Siggia ED, Cross FR. The effects of molecular noise and size control on variability in the budding yeast cell cycle. *Nature.* 2007; 448:947–951. [PubMed: 17713537]
- Wang H, Carey LB, Cai Y, Wijnen H, Futcher B. Recruitment of Cln3 Cyclin to Promoters Controls Cell Cycle Entry via Histone Deacetylase and Other Targets. *PLoS Biol.* 2009; 7:e1000189. [PubMed: 19823669]
- Vergés E, Colomina N, Garí E, Gallego C, Aldea M. Cyclin Cln3 Is Retained at the ER and Released by the J Chaperone Ydj1 in Late G1 to Trigger Cell Cycle Entry. *Mol Cell.* 2007; 26:649–662. [PubMed: 17560371]
- Tyers M, Tokiwa G, Futcher B. Comparison of the *Saccharomyces cerevisiae* G1 cyclins: Cln3 may be an upstream activator of Cln1, Cln2 and other cyclins. *The EMBO Journal.* 1993; 12:1955–1968. [PubMed: 8387915]
- Lloyd AC. The regulation of cell size. *Cell.* 2013; 154:1194–1205. [PubMed: 24034244]
- Ginzberg MB, Kafri R, Kirschner M. Cell biology. On being the right (cell) size. *Science.* 2015; 348:1245075–1245075. [PubMed: 25977557]
- Di Talia S, et al. Daughter-specific transcription factors regulate cell size control in budding yeast. *PLoS Biol.* 2009; 7:e1000221. [PubMed: 19841732]
- Johnston GC, Pringle JR, Hartwell LH. Coordination of growth with cell division in the yeast *Saccharomyces cerevisiae*. *Exp Cell Res.* 1977; 105:79–98. [PubMed: 320023]
- de Bruin RAM, McDonald WH, Kalashnikova TI, Yates J, Wittenberg C. Cln3 activates G1-specific transcription via phosphorylation of the SBF bound repressor Whi5. *Cell.* 2004; 117:887–898. [PubMed: 15210110]
- Costanzo M, et al. CDK activity antagonizes Whi5, an inhibitor of G1/S transcription in yeast. *Cell.* 2004; 117:899–913. [PubMed: 15210111]

15. Landry BD, Doyle JP, Toczyski DP, Benanti JA. F-Box Protein Specificity for G1 Cyclins Is Dictated by Subcellular Localization. *PLoS Genet.* 2012; 8:e1002851. [PubMed: 22844257]
16. Yahya G, Parisi E, Flores A, Gallego C, Aldea M. A Whi7-anchored loop controls the G1 Cdk-cyclin complex at start. *Mol Cell.* 2014; 53:115–126. [PubMed: 24374311]
17. Bhaduri S, Pryciak PM. Cyclin-specific docking motifs promote phosphorylation of yeast signaling proteins by G1/S Cdk complexes. *Curr Biol.* 2011; 21:1615–1623. [PubMed: 21945277]
18. Liu X, et al. Reliable cell cycle commitment in budding yeast is ensured by signal integration. *Elife.* 2015; 4:e03977.
19. Tyers M, Tokiwa G, Nash R, Futcher B. The Cln3-Cdc28 kinase complex of *S. cerevisiae* is regulated by proteolysis and phosphorylation. *The EMBO Journal.* 1992; 11:1773–1784. [PubMed: 1316273]
20. Fantes PA, Grant WD, Pritchard RH, Sudbery PE, Wheals AE. The regulation of cell size and the control of mitosis. *J. Theor. Biol.* 1975; 50:213–244. [PubMed: 1127959]
21. Wu C-Y, Rolfe PA, Gifford DK, Fink GR. Control of Transcription by Cell Size. *PLoS Biol.* 2010; 8:e1000523. [PubMed: 21072241]
22. Pramila T, Wu W, Miles S, Noble WS, Breeden LL. The Forkhead transcription factor Hcm1 regulates chromosome segregation genes and fills the S-phase gap in the transcriptional circuitry of the cell cycle. *Genes & development.* 2006; 20:2266–2278. [PubMed: 16912276]
23. Marguerat S, Bähler J. Coordinating genome expression with cell size. *Trends Genet.* 2012; 28:560–565. [PubMed: 22863032]
24. Epstein CB, Cross FR. Genes that can bypass the CLN requirement for *Saccharomyces cerevisiae* cell cycle START. *Molecular and cellular biology.* 1994; 14:2041–2047. [PubMed: 8114735]
25. Schneider BL, et al. Growth rate and cell size modulate the synthesis of, and requirement for, G1-phase cyclins at start. *Molecular and cellular biology.* 2004; 24:10802–10813. [PubMed: 15572683]
26. Thorburn RR, et al. Aneuploid yeast strains exhibit defects in cell growth and passage through START. *Mol Biol Cell.* 2013; 24:1274–1289. [PubMed: 23468524]
27. Shi L, Tu BP. Acetyl-CoA induces transcription of the key G1 cyclin CLN3 to promote entry into the cell division cycle in *Saccharomyces cerevisiae*. *Proc Natl Acad Sci USA.* 2013; 110:7318–7323. [PubMed: 23589851]
28. Polymenis M, Schmidt EV. Coupling of cell division to cell growth by translational control of the G1 cyclin CLN3 in yeast. *Genes & development.* 1997; 11:2522–2531. [PubMed: 9334317]
29. Menoyo S, et al. Phosphate-activated cyclin-dependent kinase stabilizes G1 cyclin to trigger cell cycle entry. *Molecular and cellular biology.* 2013; 33:1273–1284. [PubMed: 23339867]
30. Doncic A, Eser U, Atay O, Skotheim JM. An Algorithm to Automate Yeast Segmentation and Tracking. *PLoS ONE.* 2013; 8:e57970. [PubMed: 23520484]
31. Bastajian N, Friesen H, Andrews BJ. Bck2 acts through the MADS box protein Mcm1 to activate cell-cycle-regulated genes in budding yeast. *PLoS Genet.* 2013; 9:e1003507. [PubMed: 23675312]
32. Ferrezuelo F, Aldea M, Futcher B. Bck2 is a phase-independent activator of cell cycle-regulated genes in yeast. *Cell Cycle.* 2009; 8:239–252. [PubMed: 19158491]
33. Ottoz DSM, Rudolf F, Stelling J. Inducible, tightly regulated and growth condition-independent transcription factor in *Saccharomyces cerevisiae*. *Nucleic Acids Res.* 2015; 42:e130–e130. [PubMed: 25034689]
34. Miller ME, Cross FR, Groeger AL, Jameson KL. Identification of novel and conserved functional and structural elements of the G1 cyclin Cln3 important for interactions with the CDK Cdc28 in *Saccharomyces cerevisiae*. *Yeast.* 2005; 22:1021–1036. [PubMed: 16200502]
35. Miller ME, Cross FR. Mechanisms controlling subcellular localization of the G(1) cyclins Cln2p and Cln3p in budding yeast. *Molecular and cellular biology.* 2001; 21:6292–6311. [PubMed: 11509671]
36. Nash R, Tokiwa G, Anand S, Erickson K, Futcher AB. The WHI1+ gene of *Saccharomyces cerevisiae* tethers cell division to cell size and is a cyclin homolog. *The EMBO Journal.* 1988; 7:4335–4346. [PubMed: 2907481]

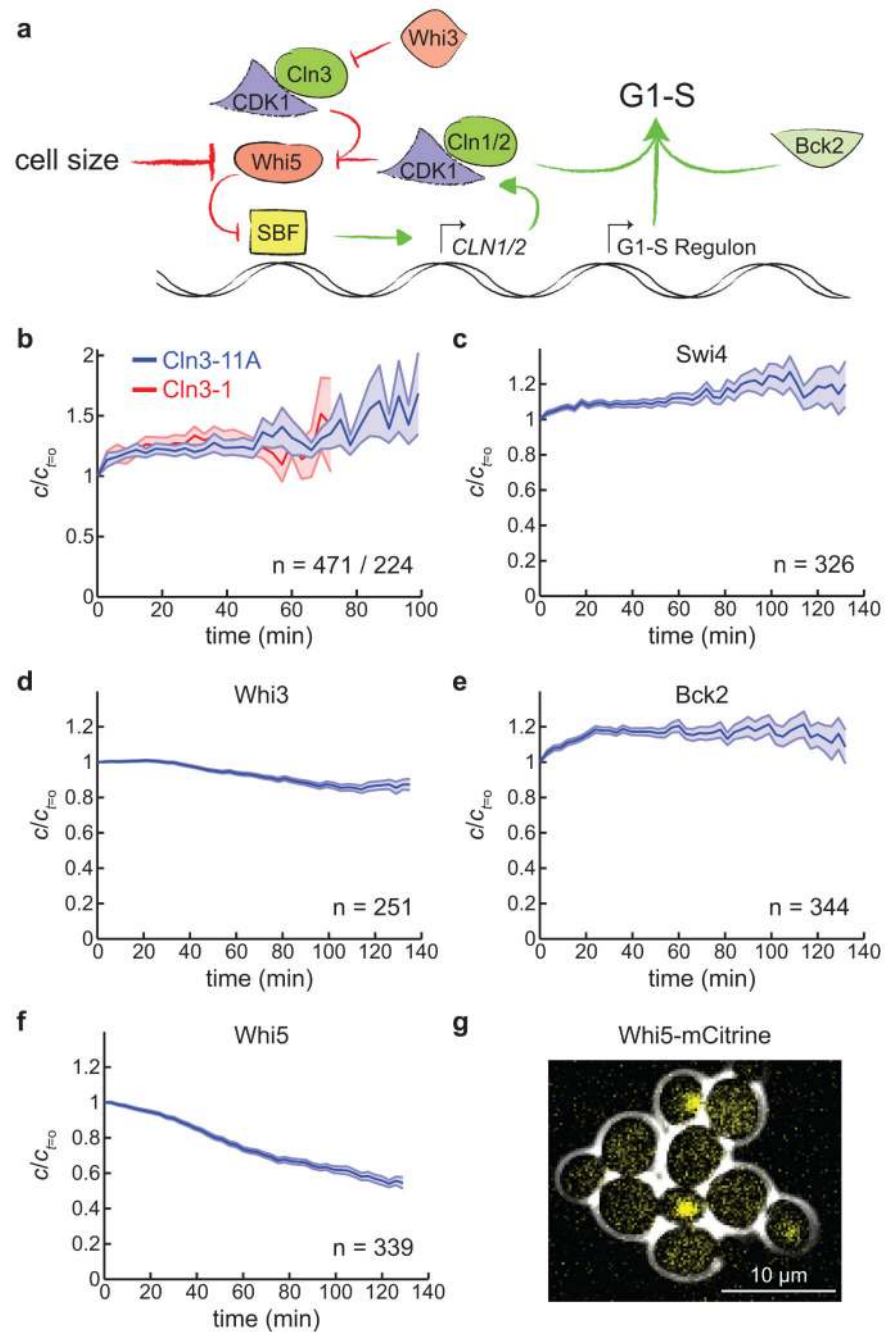


Figure 1. The cell cycle inhibitor Whi5 is diluted by growth in G1

a, Schematic of the G1/S regulatory network. **b-f**, Change in cellular protein concentration during G1 (mean \pm standard error) for daughter cells expressing the indicated protein fused to mCitrine. Concentration was normalized to the concentration at cell birth ($t=0$). **g**, Composite phase and fluorescence image of *WHI5-mCitrine* cells.

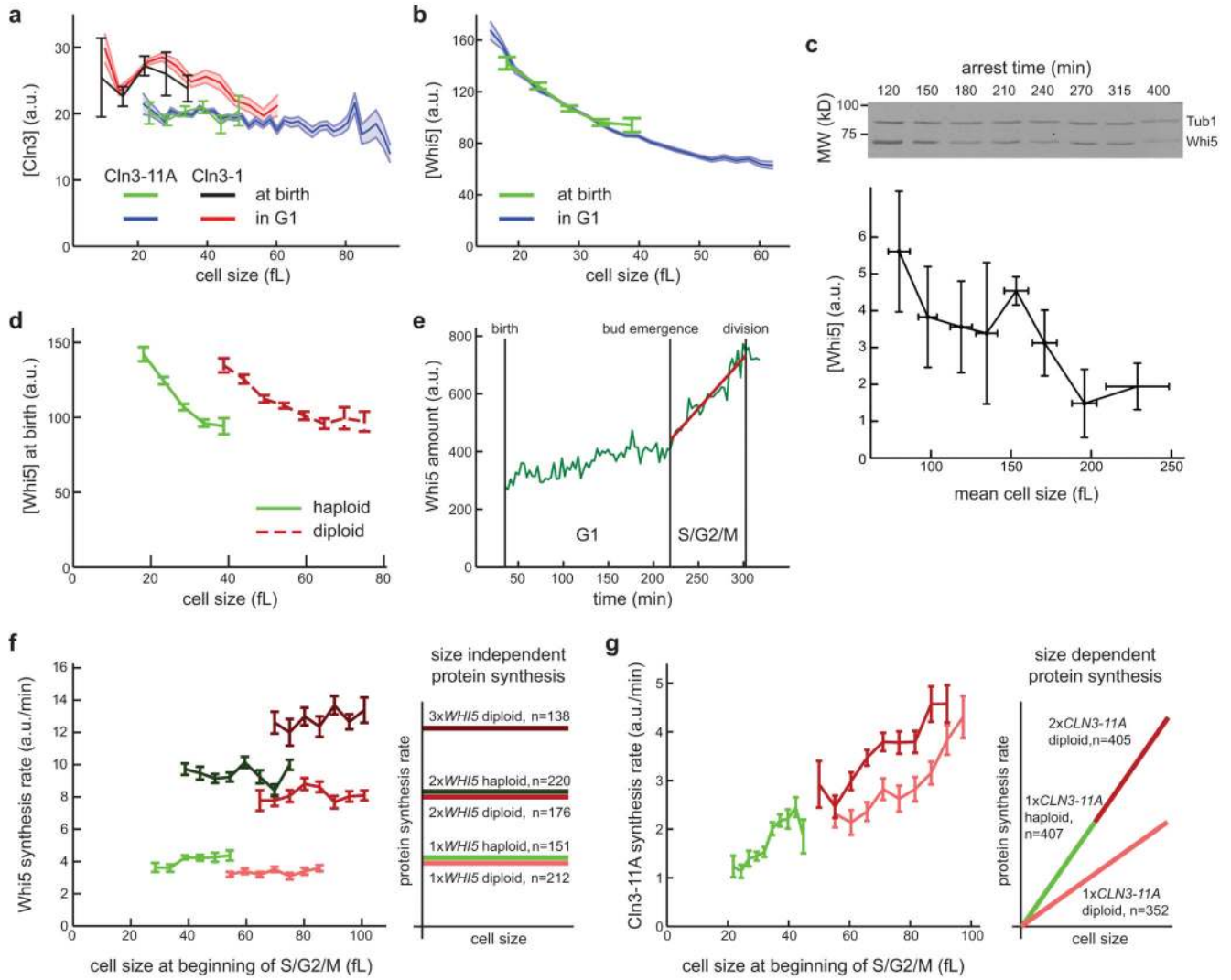


Figure 2. Differential size-dependence of Cln3 and Whi5

a-b, Mean concentration of mCitrine-Cln3-11A ($n=471$), mCitrine-Cln3-1 ($n=234$) (**a**) and Whi5-mCitrine ($n=339$) (**b**) as a function of cell size for daughter cells in G1. Shaded area indicates standard error of the mean. Bars denote mean concentration and associated standard error as a function of cell size at birth. **c**, (top) representative immunoblot of cells arrested in G1 for increasing amounts of time. (bottom) quantification of combined data from 4 independent time courses binned by mean population cell size (see methods). Bars denote mean values and standard deviation. Lanes were normalized by total protein content. Cells were grown on SCD. **d**, Mean Whi5 concentration (\pm standard error) at cell birth is shown as a function of cell size for haploid ($n=339$) and diploid ($n=385$) cells. **e**, Characteristic single-cell trace showing the total amount of Whi5-mCitrine in a haploid cell. The approximately linear increase in Whi5 during S/G2/M was fit to determine the rate of synthesis. **f-g**, Mean rate of Whi5 (**f**) and Cln3-11A (**g**) synthesis as a function of cell size for each genotype indicated in the idealized schematics. Bars denote standard errors. The rate of Cln3 synthesis is proportional to cell size as indicated by its constant concentration in

G1 shown in (a) (see Extended Data Fig. 5), whereas the Whi5 synthesis rate is largely size-independent. See Extended Data Fig. 4a-b for corresponding single cell data.

Author Manuscript

Author Manuscript

Author Manuscript

Author Manuscript

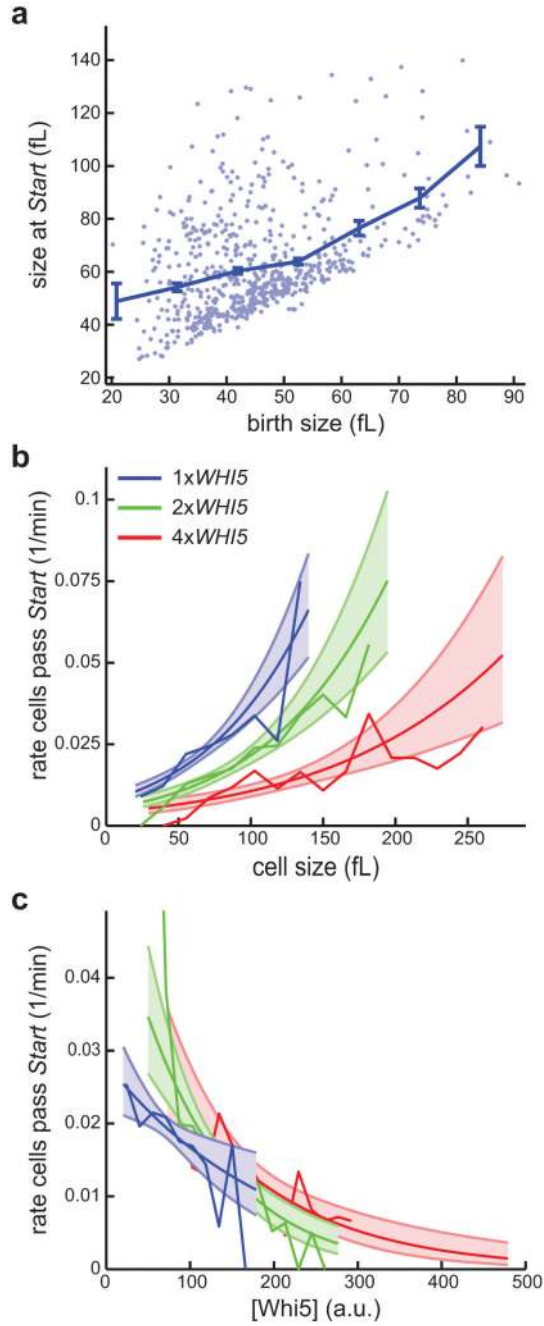


Figure 3. Whi5 concentration determines the rate at which cells progress through *Start*
a. Size at *Start*, the point of commitment to cell division, as a function of birth size for haploid *bck2Δ* daughter cells (n=658). Bars denote mean and standard error. **b-c.** The rate at which daughter cells progress through *Start* is shown as a function of cell size (**b**) and Whi5 concentration (**c**) for *bck2Δ* haploid cells with one (blue, n=658), two (green, n=310) or four (red, n=142) copies of *WHI5-mCitrine*. Smooth lines are logistic regressions and the corresponding shaded areas denote 95% confidence intervals. Jagged lines connect means for binned data.

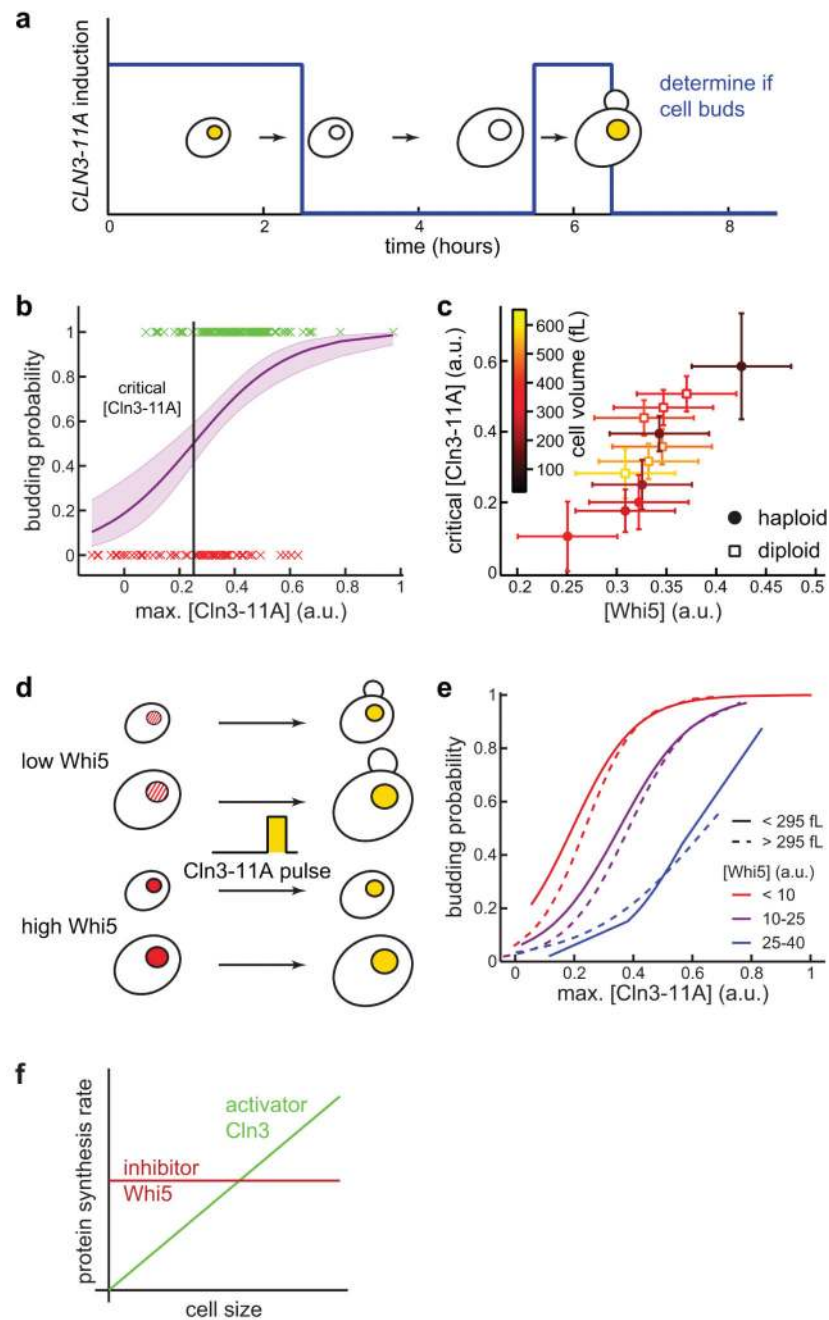


Figure 4. Cln3 and Whi5 concentrations determine the rate at which cells pass *Start* irrespective of ploidy and cell size

a. Schematic of Cln3-pulse experiments. *MET25pr-mCitrine-CLN3-11A bck2Δ* cells are arrested in G1 for 2-4 hours by addition of methionine to create G1 daughter cells of varying size. Following arrest, *mCitrine-CLN3-11A* expression is induced for varying amounts of time (0-60 minutes). **b.** Cells are binned by size and a logistic regression is then used to calculate the fraction of cells driven into the cell cycle as a function of the maximum Cln3-11A concentration produced by the exogenous pulse. Regression shown for 200-250

fL cells to determine the critical Cln3 concentration, where 50% of the cells bud. Single cell data are marked green (budding) or red (not budding). **c**, The critical Cln3-11A concentration increases with Whi5 concentration, which was determined independently for each size bin (Extended Data Fig. 8). Haploid (closed circles, n=1195) and diploid (open squares, n=405) cells show a similar relationship between Whi5 and critical Cln3-11A concentrations ($p>0.05$). **d**, To decouple cell size and Whi5 concentration, the pulse experiment is repeated with a strain expressing both *WHI5* and *CLN3-11A* from exogenously controlled promoters (MET25pr-mCitrine-CLN3-11A LexApr-WHI5-mCherry bck2 Δ). Whi5 concentration and the duration of G1 arrest prior to the Cln3 pulse are varied. **e**, Data are displayed using two size and three Whi5 concentration bins. Higher Cln3 pulse amplitudes are needed to drive cells with higher Whi5 levels into the cell cycle, while no significant difference is observed for smaller and larger cells ($p>0.5$, n=471), which we note also have different DNA concentrations. **f**, differential size-scaling of protein synthesis underlies budding yeast size control and provides a general mechanism to measure cell size independently of cell geometry.